

# <sup>213</sup>Bi-Labeled Prostate-Specific Membrane Antigen-Targeting Agents Induce DNA Double-Strand Breaks in Prostate Cancer Xenografts

Julie Nonnekens,<sup>1,2,\*</sup> Kristell L.S. Chatalic,<sup>1,3,\*</sup> Janneke D.M. Molkenboer-Kuenen,<sup>4</sup> Cecile E.M.T. Beerens,<sup>5</sup> Frank Bruchertseifer,<sup>6</sup> Alfred Morgenstern,<sup>6</sup> Joke Veldhoven-Zweistra,<sup>3</sup> Margret Schottelius,<sup>7</sup> Hans-Jürgen Wester,<sup>7</sup> Dik C. van Gent,<sup>2</sup> Wytske M. van Weerden,<sup>3</sup> Otto C. Boerman,<sup>4</sup> Marion de Jong,<sup>1</sup> and Sandra Heskamp<sup>4</sup>

## Abstract

**Background:** Up to now, prostate-specific membrane antigen (PSMA)-targeted radionuclide therapy mainly focused on  $\beta$ -emitting radionuclides. Herein, two new <sup>213</sup>Bi-labeled agents for PSMA-targeted  $\alpha$  therapy of prostate cancer (PCa) are reported.

**Methods:** The biodistribution of <sup>213</sup>Bi-labeled small-molecule inhibitor PSMA I&T and nanobody JVZ-008 was evaluated in mice bearing PSMA-positive LNCaP xenografts. DNA damage response was followed using LNCaP cells and LNCaP xenografts.

**Results:** *In vitro*, <sup>213</sup>Bi-PSMA I&T and <sup>213</sup>Bi-JVZ-008 therapy of LNCaP cells led to increased number of DNA double-strand breaks (DSBs), detected as 53BP1 and  $\gamma$ H2AX nuclear foci. *In vivo*, tumor uptake of <sup>213</sup>Bi-PSMA I&T and <sup>213</sup>Bi-JVZ-008 was  $5.75\% \pm 2.70\%ID/g$  (injected dose per gram) and  $2.68\% \pm 0.56\%ID/g$ , respectively, with similar tumor-to-kidney ratios. Furthermore, both agents induced *in vivo* DSBs in the tumors, which were detected between 1 hour and 24 hours after injection. <sup>213</sup>Bi-PSMA I&T induced significantly more DSBs than <sup>213</sup>Bi-JVZ-008 ( $p < 0.01$ ).

**Conclusions:** <sup>213</sup>Bi-PSMA I&T and <sup>213</sup>Bi-JVZ-008 showed efficient and rapid tumor targeting and produced DSBs in PSMA-expressing LNCaP cells and xenografts. These promising results require further evaluation of <sup>213</sup>Bi-labeled agents with regard to their therapeutic efficacy and toxicity for PCa therapy.

**Keywords:** Bi-213, prostate cancer, PSMA, radionuclide therapy, targeted  $\alpha$  therapy

## Introduction

Late stage metastasized prostate cancer (PCa) is associated with a poor survival and diminished quality of life. Taxane-based therapies and second-line hormonal therapies show only moderate survival benefits and are often associated with toxicity.<sup>1</sup> The recently introduced bone-seeking radiopharmaceutical radium-223 chloride (<sup>223</sup>RaCl<sub>2</sub>, Xofigo™) results in reduction of bone pain and overall survival advantage of 3.6 months in

castration-resistant PCa patients with bone metastases.<sup>2</sup> However, the use of this promising radiopharmaceutical is limited to the treatment of bone metastases. Therefore, there is an urgent need to develop a PCa-targeted  $\alpha$ -therapy approach to target and treat all PCa metastases.

Recent studies have shown that prostate-specific membrane antigen (PSMA) is an important target for radionuclide imaging and therapy of PCa. PSMA is selectively over-expressed in 90%–100% of primary and metastatic PCa

Departments of <sup>1</sup>Radiology and Nuclear Medicine, <sup>2</sup>Molecular Genetics and <sup>3</sup>Urology, Erasmus MC, Rotterdam, The Netherlands.

<sup>4</sup>Department of Radiology and Nuclear Medicine, Radboud University Medical Center, Nijmegen, The Netherlands.

<sup>5</sup>Department of Radiation Oncology, Erasmus MC, Rotterdam, The Netherlands.

<sup>6</sup>European Commission, Joint Research Centre, Directorate for Nuclear Safety and Security, Karlsruhe, Germany.

<sup>7</sup>Pharmaceutical Radiochemistry, Technische Universität München, Garching, Germany.

\*These authors contributed equally to this work.

Address correspondence to: Sandra Heskamp; Department of Radiology and Nuclear Medicine, Radboud University Medical Center; Geert Grooteplein Zuid 10, Nijmegen 6525 GA, The Netherlands  
E-mail: sandra.heskamp@radboudumc.nl

lesions.<sup>3,4</sup> Currently, several small-molecule PSMA ligands have made their way into the clinic for PCa imaging (e.g., <sup>68</sup>Ga-PSMA-11, <sup>68</sup>Ga-PSMA I&T, and <sup>18</sup>F-DCFPyl).<sup>5–7</sup> Up to now, PSMA-targeted radionuclide therapy mainly focused on  $\beta$ -emitting radionuclides. Studies with small molecule inhibitors and antibodies, such as <sup>131</sup>I-MIP-1095, <sup>177</sup>Lu-PSMA-617, <sup>177</sup>Lu-PSMA I&T, and <sup>177</sup>Lu-J591, have shown the safety and therapeutic efficacy of this approach. However, ~30% of PCa patients do not respond to these agents or develop resistance during treatment.<sup>6,8–13</sup> The therapeutic efficacy of PSMA-targeted agents could be improved using  $\alpha$ -emitting radionuclides.  $\alpha$  particles have higher energies (4–9 MeV) and shorter path lengths (40–100  $\mu$ m) than  $\beta$  particles (energy: 0.1–2.2 MeV, path length: 1–10 mm). The high linear energy transfer (LET) of  $\alpha$  particles causes complex DNA double-strand breaks (DSBs), resulting in deletions, chromosome aberrations, and cell death.<sup>14–16</sup> High LET radionuclides, therefore, have a higher biological effectiveness to kill cancer cells and may significantly enhance the efficacy of radionuclide therapy.<sup>17,18</sup> First in-human studies of PSMA-617 labeled with the long-lived  $\alpha$  emitter <sup>225</sup>Ac ( $t_{1/2}$ =9.9 days) have shown remarkable therapeutic efficacy in PCa patients resistant to <sup>177</sup>Lu-PSMA or in whom treatment with  $\beta$  emitters was contraindicated because of diffuse red marrow infiltration.<sup>19</sup>

Here two PSMA-targeting tracers are evaluated, PSMA I&T and the nanobody JVZ-008, coupled to the  $\alpha$  emitter <sup>213</sup>Bi. <sup>213</sup>Bi ( $t_{1/2}$ =46 minutes) decays to stable <sup>209</sup>Bi with a branching of 97.8% through the emission of a  $\beta^-$  particles to <sup>213</sup>Po, immediately followed by the emission of the main therapeutically relevant  $\alpha$  particle of 8.4 MeV. With a branching of 2.2%, <sup>213</sup>Bi decays through the emission of an  $\alpha$  particle with 5.9 MeV to <sup>209</sup>Tl, followed by the emission of a  $\beta^-$  particle to stable <sup>209</sup>Bi.<sup>20</sup> PSMA I&T and JVZ-008 are directed against the extracellular domain of PSMA and show rapid accumulation in PSMA-expressing tumors and represent ideal molecular carriers for the short-lived <sup>213</sup>Bi.<sup>6,13,21,22</sup> The aim of this study is to assess the tumor targeting and biodistribution profiles of <sup>213</sup>Bi-PSMA I&T and <sup>213</sup>Bi-JVZ-007-cys-DOTA (<sup>213</sup>Bi-JVZ-008), as well as the resulting induction of DSBs using the PSMA-expressing human PCa xenograft model LNCaP.

## Materials and Methods

All reagents used were purchased from Sigma-Aldrich BV, The Netherlands, unless stated otherwise.

### Synthesis and radiolabeling of <sup>213</sup>Bi-PSMA I&T and <sup>213</sup>Bi-JVZ-008

PSMA I&T was kindly provided by the Technical University Munich and JVZ-007-cys was synthesized as described previously.<sup>6,22</sup> JVZ-008 was obtained by conjugation of JVZ-007-cys to maleimide-1,4,7,10-tetraazacyclododecane-1,4,7,10-tetraacetic acid (DOTA, Chematech, Dijon, France) according to the protocol described for maleimide-maleimide-diethylene-triaminepentaacetic acid (DTPA).<sup>22</sup> <sup>213</sup>Bi was eluted as BiI<sub>4</sub><sup>-</sup>/BiI<sub>5</sub><sup>2-</sup> from a <sup>225</sup>Ac/<sup>213</sup>Bi generator produced by the Directorate for Nuclear Safety and Security (Karlsruhe, Germany), using 600  $\mu$ L of 0.1 M HCl/0.1 M NaI. For PSMA I&T labeling, the <sup>213</sup>Bi eluate was added to a labeling vial containing 120  $\mu$ L of 2 M Tris, 50  $\mu$ L of 20% ascorbic acid and 2–4 nmol PSMA I&T (pH 8.7). For JVZ-008 labeling, the <sup>213</sup>Bi eluate was added to a labeling vial containing 80  $\mu$ L of 2 M Tris,

50  $\mu$ L of 20% ascorbic acid, and 4 nmol JVZ-008 (pH 7.9). The reaction mixture was heated for 10 minutes at 95°C. After the reaction, DTPA was added to a final concentration of 0.03 mM to complex-free <sup>213</sup>Bi. Incorporation yield was determined by instant thin-layer chromatography (Agilent Technologies) using 0.1 M NH<sub>4</sub>OAc/0.1 M EDTA (pH 5.5) and 0.1 M sodium citrate (pH 6.0) as eluent for <sup>213</sup>Bi-PSMA I&T and <sup>213</sup>Bi-JVZ-008, respectively. Radioactivity corresponding to <sup>213</sup>Bi-PSMA I&T (Rf=0.5), <sup>213</sup>Bi-JVZ-008 (Rf=0), and free <sup>213</sup>Bi (Rf=1) was quantified using a gamma counter (Perkin Elmer). Incorporation yield always exceeded 95%.

For animal experiments, radiolabeled tracers were purified and formulated in a physiological buffer. <sup>213</sup>Bi-PSMA I&T was purified using an Oasis<sup>TM</sup> HLB column (Waters, Milford, MA) preconditioned with 1 mL ethanol and 2 mL water. <sup>213</sup>Bi-PSMA I&T was loaded on the column and eluted with 500  $\mu$ L ethanol. The volume was reduced to 50  $\mu$ L by evaporation, 50 nmol 2-(phosphonomethyl)pentane-1,5-dioic acid (PMPA; Santa Cruz Biotechnology, Dallas, TX) was added and phosphate-buffered saline (PBS)/0.5% bovine serum albumin (BSA) was added up to 1 mL. Mice received 200  $\mu$ L of this solution. <sup>213</sup>Bi-JVZ-008 was purified by size exclusion chromatography using an illustra NAP-5 column (GE Healthcare Life Sciences, The Netherlands) preconditioned with 5 volumes of 0.5% BSA and eluted with 1 mL PBS in 100  $\mu$ L fractions. The first five fractions were pooled and mice were coinjected with 100  $\mu$ L of this solution combined with 100  $\mu$ L gelofusine (40 mg/mL). Specific activity was 30 MBq/nmol and 7 MBq/nmol at time of injection for <sup>213</sup>Bi-PSMA I&T and <sup>213</sup>Bi-JVZ-008, respectively.

### Cell culture

The human PCa cell line LNCaP was cultured in RPMI1640 (GIBCO, BRL Life Sciences Technologies, The Netherlands), with 2 mM glutamine (GIBCO) and 10% fetal calf serum (at 37°C with 5% CO<sub>2</sub>).

*In vitro* experiments. LNCaP cells were seeded in 12-well plates (5  $\times$  10<sup>4</sup> cells in 1 mL/well) on sterile 13-mm diameter cover slips and allowed to grow for 2 days. Subsequently, cells were treated for 20 minutes at 37°C with 300  $\mu$ L of <sup>213</sup>Bi-PSMA I&T (10<sup>-7</sup> M, 0.3 MBq), <sup>213</sup>Bi-JVZ-008 (10<sup>-7</sup> M, 0.3 MBq), nontargeted tracer <sup>213</sup>Bi-DTPA (2  $\times$  10<sup>-6</sup> M, 0.3 MBq), or medium containing labeling buffer. Immediately after treatment, cells were washed with 1 mL PBS and incubated with normal medium for 1, 2, 4, 24, or 48 hours. After incubation, cells were washed with 2 mL PBS, fixed for 15 minutes in 0.5 mL of 2% paraformaldehyde at room temperature (RT), and washed with 1 mL PBS.

*In vivo* experiments. All animal experiments were conducted in accordance with the revised Dutch Act on Animal Experimentation (1997) and approved by the institutional Animal Welfare Committee of the Radboud University Nijmegen.

Female nude BALB/c mice (4 animals per condition, age 6–8 weeks; Janvier Lab, Le Genest-Saint-Isle, France) were inoculated subcutaneously with LNCaP cells (3  $\times$  10<sup>6</sup> cells, 200  $\mu$ L, 33% RPMI/67% matrigel, BD Biosciences, Pharmingen, San. Diego, CA). Three weeks after inoculation (tumors 4–5 mm in diameter), <sup>213</sup>Bi-PSMA I&T (0.2 nmol, 5.4–6.6 MBq) was injected intravenously with 10 nmol

2-PMPA for renal protection and  $^{213}\text{Bi}$ -JVZ-008 (0.7 nmol, 4.5–5.4 MBq) was injected intravenously with 4 mg gefosine for renal protection.<sup>21,23</sup> Nontreated animals were taken along as controls.

At 1 and 24 hours after injection, mice were euthanized using  $\text{CO}_2/\text{O}_2$  asphyxiation and tumor, blood, muscle, lung, spleen, kidney, liver, small intestine, colon, and salivary glands were collected and weighed. Tumors were fixed in 4% paraformaldehyde. For biodistribution studies at 1 hour after injection, radioactivity in each organ was determined in a  $\gamma$  counter by measuring the  $\gamma$  emission of  $^{213}\text{Bi}$  (440 keV), and the percentage of the injected dose per gram (%ID/g) was calculated. After radioactive decay (>10 half-lives), fixed tissues were embedded in paraffin.

#### Immunofluorescence staining cells

Phosphorylation of histone H2AX ( $\gamma\text{H2AX}$ ) and accumulation of p53-binding protein 1 (53BP1) at the site of DSBs are biomarkers of radiation-induced DSBs.<sup>24</sup> Fixed LNCaP cells were permeabilized for 20 minutes at RT in PBS containing 0.1% Triton X-100 and incubated in blocking buffer (PBS, 0.1% Triton X-100, 2% BSA) for 30 minutes at RT. Next, cells were stained for 90 minutes at RT with primary antibodies [anti-53BP1 (NB100-304, dilution 1/1000; Novus Biologicals, Littleton, CO) and anti- $\gamma\text{H2AX}$  (05-636, dilution 1/500; Merck-Millipore, Billerica, Massachusetts)] diluted in blocking buffer. After incubation, cells were washed with PBS 0.1% Triton X-100 and incubated with the secondary antibody (goat antirabbit Alexa Fluor 594 or goat antimouse Alexa Fluor 488, 1/1000; Thermo Fisher Scientific, Waltham, MA) in blocking buffer for 60 minutes at RT. Cells were washed with PBS and mounted with Vectashield containing DAPI (Vector Laboratories, Burlingame, CA). Fluorescent Z-stack imaging was performed using a TCS SP5 confocal microscope (Leica, Wetzlar, Germany).

#### Immunofluorescence staining tumor tissue

For analysis of *in vivo* DSBs induction, tumors were paraffin embedded. Four micrometer tissue sections were deparaffinized in xylene and subsequently rehydrated by incubation in decreasing concentrations of ethanol. Target antigen retrieval was performed using a Target Retrieval Solution pH6.1 (Agilent Technologies, Santa Clara, CA) for 18 minutes in a microwave at 650 W. Immunofluorescent stainings and imaging were performed as described for cells. Pictures were processed using the Temporal-Color Code mode from Image J software. Manual  $\alpha$  tracks quantification of on average 375 cells of 4 animals per condition was performed. Foci are considered to form an  $\alpha$  track when they are observed as a line or when at least four foci lay in the same line within a nucleus.

#### Statistical analysis

Statistical analyses were performed using PASW Statistics version 22.0 (Chicago, IL). Differences in tracer uptake were tested for significance using the nonparametric Mann-Whitney U test. Differences in number of  $\alpha$  tracks were determined using a homoscedastic two-tailed Student's *t*-test. Samples were considered statistically different if  $p < 0.05$  with  $**p < 0.01$  and  $***p < 0.001$ .

## Results

### $^{213}\text{Bi}$ -radiolabeling of PSMA I&T and JVZ-008

The labeling procedure is depicted in Supplementary Figure S1 (Supplementary Data are available online at [www.liebertpub.com/cbr](http://www.liebertpub.com/cbr)). Radiolabeling with  $^{213}\text{Bi}$  was achieved within 15 minutes with a specific activity (nondecay corrected) of 58 MBq/nmol and 29 MBq/nmol for  $^{213}\text{Bi}$ -PSMA I&T and  $^{213}\text{Bi}$ -JVZ-008, respectively. The incorporation yield was >95%.

### $^{213}\text{Bi}$ -PSMA I&T and $^{213}\text{Bi}$ -JVZ-008 induce DSBs in LNCaP cells in vitro

Therapy with the PSMA-targeted tracers  $^{213}\text{Bi}$ -PSMA I&T and  $^{213}\text{Bi}$ -JVZ-008 and the nontargeted tracer  $^{213}\text{Bi}$ -DTPA all induced DSBs in LNCaP cells, as shown by the presence of 53BP1 and  $\gamma\text{H2AX}$  foci (Figure 1 and Supplementary Fig. S2). At early time points, both single foci and linear tracks, that is,  $\alpha$  tracks, were visible. Tracks were present at least until 4 hours after treatment, but were not observed anymore at 24 and 48 hours after treatment. Single DSB foci were still present at these later time points. Background 53BP1 and  $\gamma\text{H2AX}$  nuclear foci, most likely arising from replication stress, were observed in vehicle-treated LNCaP cells.

### $^{213}\text{Bi}$ -PSMA I&T and $^{213}\text{Bi}$ -JVZ-008 accumulate in LNCaP tumors in mice

$^{213}\text{Bi}$ -PSMA I&T and  $^{213}\text{Bi}$ -JVZ-008 accumulated in LNCaP tumors and in kidneys (Fig. 2). Tumor uptake was  $5.75\% \pm 2.70\% \text{ID/g}$  and  $2.68\% \pm 0.56\% \text{ID/g}$  for  $^{213}\text{Bi}$ -PSMA I&T and  $^{213}\text{Bi}$ -JVZ-008, respectively (1 hour after injection,  $p = 0.057$ ). Both tracers cleared rapidly from blood ( $^{213}\text{Bi}$ -PSMA I&T:  $0.30\% \pm 0.21\% \text{ID/g}$  and  $^{213}\text{Bi}$ -JVZ-008:  $0.30\% \pm 0.06\% \text{ID/g}$ ).  $^{213}\text{Bi}$ -PSMA I&T showed higher kidney uptake than  $^{213}\text{Bi}$ -JVZ-008 ( $p = 0.029$ ). However, tumor-to-kidney ratios of both compounds were similar ( $^{213}\text{Bi}$ -PSMA I&T:  $0.19 \pm 0.10$  and  $^{213}\text{Bi}$ -JVZ-008:  $0.17 \pm 0.01$ ). Furthermore, uptake of  $^{213}\text{Bi}$ -PSMA I&T was observed in the spleen ( $2.12\% \pm 0.23\% \text{ID/g}$ ).

### $^{213}\text{Bi}$ -PSMA I&T and $^{213}\text{Bi}$ -JVZ-008 induce DSBs in LNCaP tumors in mice

DSBs were induced in LNCaP tumors by both  $^{213}\text{Bi}$ -PSMA I&T and  $^{213}\text{Bi}$ -JVZ-008, as reflected by increased number of 53BP1 and  $\gamma\text{H2AX}$  foci 1 hour after injection, compared with nontreated mice (Fig. 3A and Supplementary Fig. S3). A large fraction of cells with  $\alpha$  tracks were observed shortly after treatment; in  $^{213}\text{Bi}$ -PSMA I&T-treated animals, significantly more  $\alpha$  tracks in the tumors ( $20.91\% \pm 1.23\%$ ) were observed than in  $^{213}\text{Bi}$ -JVZ-008-treated animals ( $15.30\% \pm 1.07\%$ ) (Fig. 3B). Most of the  $\alpha$  tracks disappeared 24 hours after injection, but a small portion of the cells still contained these tracks ( $2.51\% \pm 0.21\%$  for  $^{213}\text{Bi}$ -PSMA I&T and  $2.43\% \pm 0.34\%$  for  $^{213}\text{Bi}$ -JVZ-008). Moreover, separate DSBs were still observed 24 hours after injection.

## Discussion

Here, the preclinical results focusing on DNA damage induction by PSMA-targeted  $\alpha$  radionuclide therapy with two novel PSMA-targeting agents are reported: the small-molecule

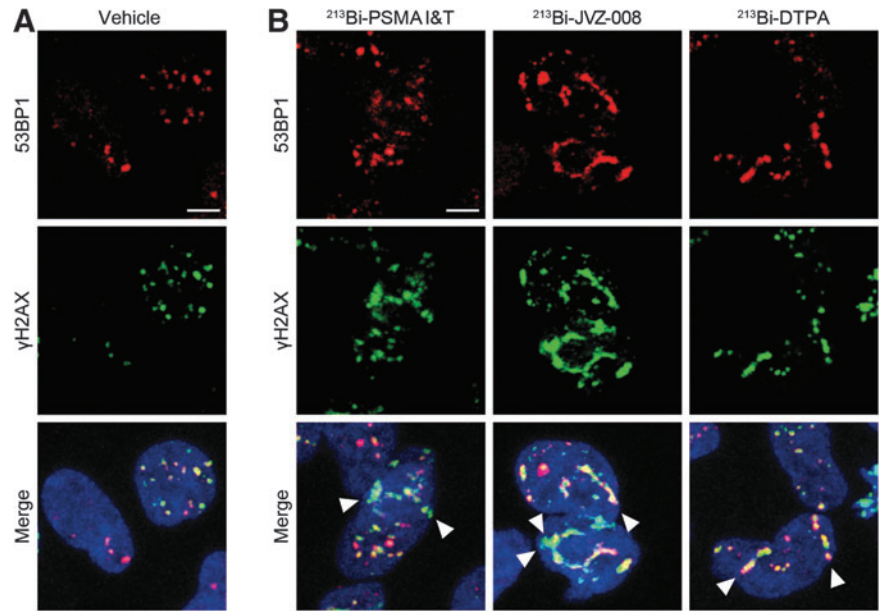


**FIG. 1.** Representative pictures of DNA double-strand breaks (visualized by immunofluorescent staining of  $\gamma$ H2AX and 53BP1) in LNCaP cells at 1 hour after treatment with vehicle (A) or at 1 hour (B) and 24 hours (C) after treatment with  $^{213}\text{Bi}$  tracers (scale bar =  $5\ \mu\text{m}$ ). Merge is an overlay of  $\gamma$ H2AX (green), 53BP1 (red), and DAPI (blue) images. Arrowheads indicate  $\alpha$  tracks.

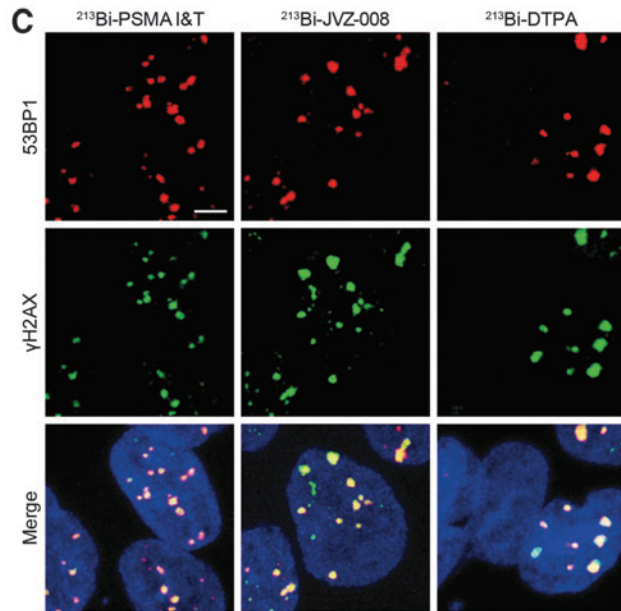
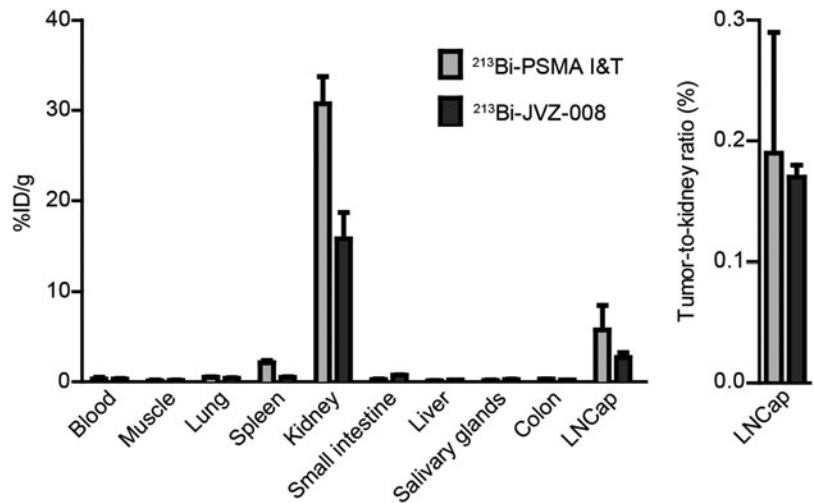


**FIG. 2.** *Ex vivo* biodistribution of  $^{213}\text{Bi}$ -PSMA I&T and  $^{213}\text{Bi}$ -JVZ-008 in LNCaP xenografts at 1 hour after injection. Uptake was measured as percentage of injected dose per gram (%ID/g). Error bars represent the SD. PSMA, prostate-specific membrane antigen; SD, standard deviation.



PSMA inhibitor  $^{213}\text{Bi}$ -PSMA I&T and the anti-PSMA nanobody  $^{213}\text{Bi}$ -JVZ-008.  $^{213}\text{Bi}$ -PSMA I&T and  $^{213}\text{Bi}$ -JVZ-008 showed rapid and efficient tumor targeting and produced DSBs in PSMA-positive LNCaP tumors *in vivo*.

Recently, several other preclinical studies have reported on PSMA-targeted radionuclide therapy using  $\alpha$ -emitting radionuclides. *In vitro* and *in vivo* treatment with the monoclonal antibody J591 labeled with  $^{213}\text{Bi}$  showed promising results.<sup>25,26</sup> However, *in vivo* application of this tracer appeared challenging because the short  $^{213}\text{Bi}$  half-life does not match with slow antibody pharmacokinetics. Two studies showed that anti-PSMA-targeted liposomes/lipid vesicles loaded with the  $\alpha$  emitter  $^{225}\text{Ac}$  can kill PSMA-expressing cells *in vitro*.<sup>27,28</sup> However, because of the high recoil energy, Ac-225 daughter products are released from the carrier. Therefore, stability and normal tissue toxicity of these radiotracers should be addressed.<sup>29</sup> A study by Kiess et al. showed the potential of  $^{211}\text{At}$ -6 *in vitro* and *in vivo* treatment,<sup>30</sup> but  $^{211}\text{At}$  was reported to lose therapeutic efficacy with increasing tumor size.<sup>31</sup> Therefore, an optimal combination between a short-lived  $\alpha$  emitter and PSMA ligand to induce DNA damage is explored. PSMA I&T and JVZ-008 show rapid accumulation in PSMA-expressing tumors (<1 hour) and, therefore, represent ideal molecular carriers

for the short-lived  $^{213}\text{Bi}$ . In this study, for the first time the application of  $^{213}\text{Bi}$  with these low-molecular weight PSMA-targeting agents is shown.

$^{213}\text{Bi}$ -PSMA I&T and  $^{213}\text{Bi}$ -JVZ-008 therapy of LNCaP cells resulted in production of DSBs, both *in vitro* and *in vivo*. However, induction of DSBs was also observed *in vitro* after treatment with the nontargeted agent  $^{213}\text{Bi}$ -DTPA, with similar DSB repair kinetics as  $^{213}\text{Bi}$ -PSMA I&T and  $^{213}\text{Bi}$ -JVZ-008. This suggests that DNA damage was induced by  $^{213}\text{Bi}$  from the medium during the 20 minutes incubation period. Because of the high cytotoxicity of  $^{213}\text{Bi}$  and its short half-life, this *in vitro* model appeared suboptimal and the tracers were further evaluated *in vivo*.

In the xenograft model, a twofold higher tumor uptake was observed for  $^{213}\text{Bi}$ -PSMA I&T than for  $^{213}\text{Bi}$ -JVZ-008 with a similar tumor-to-kidney ratio. The biodistribution of  $^{213}\text{Bi}$ -PSMA I&T and  $^{213}\text{Bi}$ -JVZ-008 was comparable with that of  $^{111}\text{In}$ - and  $^{177}\text{Lu}$ -labeled tracers.<sup>21,22</sup>  $^{213}\text{Bi}$ -PSMA I&T showed significantly higher uptake in the kidneys than  $^{213}\text{Bi}$ -JVZ-008. Both tracers are cleared through the kidneys. However, the uptake of  $^{213}\text{Bi}$ -PSMA I&T seems to be PSMA mediated, because it can be blocked by coinjecting an excess of unlabeled PSMA I&T or 2-PMPA, and not by gelofusin.<sup>21</sup> In contrast,  $^{213}\text{Bi}$ -JVZ-008 uptake can be

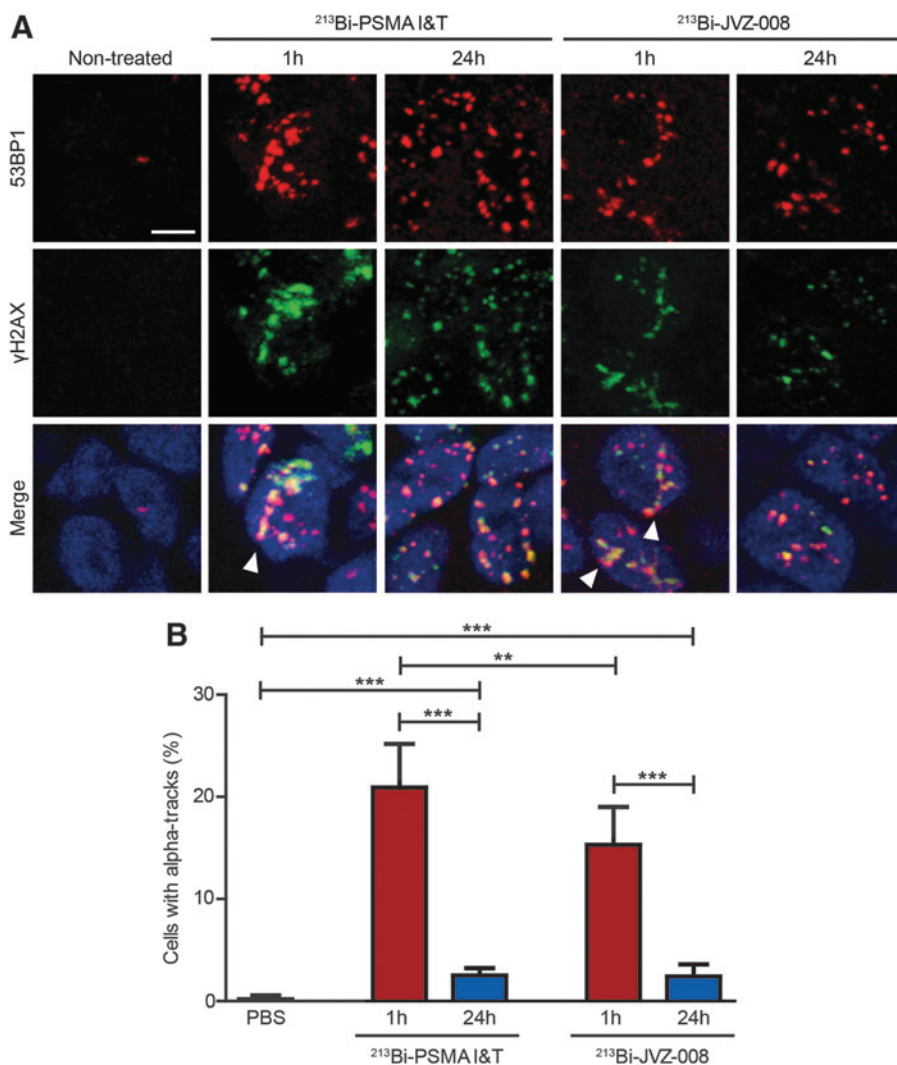


**FIG. 3.** (A) Representative pictures of DNA double-strand breaks (visualized by immunofluorescent staining of  $\gamma\text{H2AX}$  and 53BP1) in LNCaP xenografts of PBS-treated mice and 1 and 24 hours after injection of  $^{213}\text{Bi}$ -PSMA I&T or  $^{213}\text{Bi}$ -JVZ-008 (scale bar = 5  $\mu\text{m}$ ). Merge is an overlay of  $\gamma\text{H2AX}$  (green), 53BP1 (red), and DAPI (blue) images. Arrowheads indicate  $\alpha$  tracks. (B) Quantification of cells with  $\alpha$  tracks compared with the total cell population of on average 375 cells of 4 animals per condition. Error bars represent the SD. Statistics: \*\* $p < 0.01$  and \*\*\* $p < 0.001$ . PSMA, prostate-specific membrane antigen; PBS, phosphate-buffered saline; SD, standard deviation.

blocked by coinjecting gelifosin.<sup>22</sup> So far, no studies have been carried out to assess the effect of coinjection of 2-PMPA or an excess of unlabeled JVZ-008.

The higher uptake of <sup>213</sup>Bi-PSMA I&T in the tumor correlated with a significant increase in the number of cells with  $\alpha$  tracks after <sup>213</sup>Bi-PSMA I&T compared with <sup>213</sup>Bi-JVZ-008. The number of cells with  $\alpha$  tracks was significantly reduced at 24 hours after treatment for both tracers, indicating that a fraction of the DSBs in the tracks was repaired and/or that the chromatin was rearranged. These first results indicate that <sup>213</sup>Bi-PSMA I&T is more potent to induce DNA damage in the tumor, but because kidney uptake is also enhanced, nephrotoxicity needs to be monitored closely in the future.

For clinical translation, it is important to note that PSMA is also expressed in normal tissues, and dosimetric calculations for  $\beta$  emitters predict the highest absorbed doses in salivary glands and kidneys.<sup>8,32</sup> So far, only one study reported on clinical use of PSMA-targeted  $\alpha$  therapy. In 2 PCa patients, <sup>225</sup>Ac-PSMA-617 induced prostate-specific antigen decline and complete imaging response while no relevant hematological toxicity was observed. However, patients did report moderate to severe xerostomia.<sup>19</sup> Furthermore, <sup>213</sup>Bi-labeled DOTATOC has been shown to be effective in patients with neuroendocrine tumors refractory to <sup>90</sup>Y- and <sup>177</sup>Lu-DOTATOC. Although the safety profile was acceptable, patients experienced moderate acute hematological toxicity and moderate chronic kidney toxicity.<sup>33</sup>

In conclusion, <sup>213</sup>Bi-PSMA I&T and <sup>213</sup>Bi-JVZ-008 showed efficient and rapid tumor targeting and produced DSBs in PSMA-expressing LNCaP tumors. These results require further evaluation of therapeutic efficacy and toxicity. Potentially, these novel tracers could offer a promising new treatment option for PCa patients with metastatic lesions.

### Acknowledgments

The authors thank Bianca Lemmers-van de Weem, Iris Lamers-Elmans, Kitty Lemmens-Hermans, and Sharon Wenekers for their assistance during animal experiments. Fluorescent imaging was performed in collaboration with the optical imaging center of the Erasmus MC. This study was supported by the Erasmus MC grant “Novel Radio-Antagonists for PET/MRI Imaging and Therapy of Prostate Cancer” and The Netherlands Organization for Scientific Research (ZON-MW grant 40-42600-98-018).

### Disclosure Statement

No conflicting financial interests exist.

### References

1. Heidenreich A, Bastian PJ, Bellmunt J, et al. EAU guidelines on prostate cancer. Part II: Treatment of advanced, relapsing, and castration-resistant prostate cancer. *Eur Urol* 2014;65:467.
2. Parker C, Nilsson S, Heinrich D, et al. Alpha emitter radium-223 and survival in metastatic prostate cancer. *N Engl J Med* 2013;369:213.
3. Minner S, Wittmer C, Graefen M, et al. High level PSMA expression is associated with early PSA recurrence in surgically treated prostate cancer. *Prostate* 2011;71:281.

4. Silver DA, Pellicer I, Fair WR, et al. Prostate-specific membrane antigen expression in normal and malignant human tissues. *Clin Cancer Res* 1997;3:81.
5. Szabo Z, Mena E, Rowe SP, et al. Initial evaluation of [F]DCFPyL for Prostate-Specific Membrane Antigen (PSMA)-Targeted PET Imaging of Prostate Cancer. *Mol Imaging Biol* 2015;17:565–574.
6. Weineisen M, Schottelius M, Simecek J, et al. 68Ga- and 177Lu-Labeled PSMA I&T: Optimization of a PSMA-targeted theranostic concept and first proof-of-concept human studies. *J Nucl Med* 2015;56:1169.
7. Afshar-Oromieh A, Avtzi E, Giesel FL, et al. The diagnostic value of PET/CT imaging with the (68)Ga-labelled PSMA ligand HBED-CC in the diagnosis of recurrent prostate cancer. *Eur J Nucl Med Mol Imaging* 2015;42:197.
8. Herrmann K, Bluemel C, Weineisen M, et al. Biodistribution and radiation dosimetry for a probe targeting prostate-specific membrane antigen for imaging and therapy. *J Nucl Med* 2015;56:855.
9. Zechmann CM, Afshar-Oromieh A, Armor T, et al. Radiation dosimetry and first therapy results with a (124)I/(131)I-labeled small molecule (MIP-1095) targeting PSMA for prostate cancer therapy. *Eur J Nucl Med Mol Imaging* 2014;41:1280.
10. Kratochwil C, Giesel FL, Stefanova M, et al. PSMA-targeted radionuclide therapy of metastatic castration-resistant prostate cancer with Lu-177 labeled PSMA-617. *J Nucl Med* 2016;57:1170–1176.
11. Rahbar K, Schmidt M, Heinzel A, et al. Response and tolerability of a single dose of 177Lu-PSMA-617 in patients with metastatic castration-resistant prostate cancer: A multicenter retrospective analysis. *J Nucl Med* 2016;57:1334–1338.
12. Tagawa ST, Milowsky MI, Morris M, et al. Phase II study of Lutetium-177-labeled anti-prostate-specific membrane antigen monoclonal antibody J591 for metastatic castration-resistant prostate cancer. *Clin Cancer Res* 2013;19:5182.
13. Heck MM, Retz M, D'Alessandria C, et al. Systemic radioligand therapy with 177Lu labeled prostate specific membrane antigen ligand for imaging and therapy in patients with metastatic castration resistant prostate cancer. *J Urol* 2016;196:382–391.
14. Milenic DE, Brady ED, Brechbiel MW. Antibody-targeted radiation cancer therapy. *Nat Rev Drug Discov* 2004;3:488.
15. Ritter MA, Cleaver JE, Tobias CA. High-LET radiations induce a large proportion of non-rejoining DNA breaks. *Nature* 1977;266:653.
16. Nikitaki Z, Nikolov V, Mavragani IV, et al. Measurement of complex DNA damage induction and repair in human cellular systems after exposure to ionizing radiations of varying linear energy transfer (LET). *Free Radic Res* 2016;50(sup1):S64.
17. Rydberg B, Cooper B, Cooper PK, et al. Dose-dependent misrejoining of radiation-induced DNA double-strand breaks in human fibroblasts: Experimental and theoretical study for high- and low-LET radiation. *Radiat Res* 2005;163:526.
18. Mulford DA, Scheinberg DA, Jurcic JG. The promise of targeted {alpha}-particle therapy. *J Nucl Med* 2005;46 Suppl 1:199S.
19. Kratochwil C, Bruchertseifer F, Giesel FL, et al. 225Ac-PSMA-617 for PSMA targeting alpha-radiation therapy of patients with metastatic castration-resistant prostate cancer. *J Nucl Med* 2016;57:1941–1944.

20. Marouli M, Suliman G, Pomme S, et al. Decay data measurements on  $^{213}\text{Bi}$  using recoil atoms. *Appl Radiat Isot* 2013;74:123.
21. Chatalic KL, Heskamp S, Konijnenberg M, et al. Towards personalized treatment of prostate cancer: PSMA I&T, a promising prostate-specific membrane antigen-targeted theranostic agent. *Theranostics* 2016;6:849.
22. Chatalic KL, Veldhoven-Zweistra J, Bolkestein M, et al. A Novel (1)(1)(1)In-Labeled Anti-Prostate-Specific Membrane Antigen Nanobody for Targeted SPECT/CT Imaging of Prostate Cancer. *J Nucl Med* 2015;56:1094.
23. Kratochwil C, Giesel FL, Leotta K, et al. PMPA for nephroprotection in PSMA-targeted radionuclide therapy of prostate cancer. *J Nucl Med* 2015;56:293.
24. Sak A, Stuschke M. Use of gammaH2AX and other biomarkers of double-strand breaks during radiotherapy. *Semin Radiat Oncol* 2010;20:223.
25. Li Y, Tian Z, Rizvi SM, et al. In vitro and preclinical targeted alpha therapy of human prostate cancer with Bi-213 labeled J591 antibody against the prostate specific membrane antigen. *Prostate Cancer Prostatic Dis* 2002; 5:36.
26. Ballangrud AM, Yang WH, Charlton DE, et al. Response of LNCaP spheroids after treatment with an alpha-particle emitter ( $^{213}\text{Bi}$ )-labeled anti-prostate-specific membrane antigen antibody (J591). *Cancer Res* 2001;61:2008.
27. Bandekar A, Zhu C, Jindal R, et al. Anti-prostate-specific membrane antigen liposomes loaded with  $^{225}\text{Ac}$  for potential targeted antivascular alpha-particle therapy of cancer. *J Nucl Med* 2014;55:107.
28. Zhu C, Bandekar A, Sempkowski M, et al. Nanoconjugation of PSMA-targeting ligands enhances perinuclear localization and improves efficacy of delivered alpha-particle emitters against tumor endothelial analogues. *Mol Cancer Ther* 2016;15:106.
29. de Kruijff RM, Wolterbeek HT, Denkova AG. A critical review of alpha radionuclide therapy-how to deal with recoiling daughters? *Pharmaceuticals (Basel)* 2015;8:321.
30. Kiess A, Minn IL, Vaidyanathan G, et al. (2S)-2-(3-(1-Carboxy-5-(4-[ $^{211}\text{At}$ ]astatobenzamido)pentyl)ureido)-pentanedioic acid for PSMA-targeted alpha-particle radiopharmaceutical therapy. *J Nucl Med* 2016;57:1569–1575.
31. Elgqvist J, Andersson H, Back T, et al. Alpha-radioimmunotherapy of intraperitoneally growing OVCAR-3 tumors of variable dimensions: Outcome related to measured tumor size and mean absorbed dose. *J Nucl Med* 2006;47: 1342.
32. Delker A, Fendler WP, Kratochwil C, et al. Dosimetry for ( $^{177}\text{Lu}$ )-DKFZ-PSMA-617: A new radiopharmaceutical for the treatment of metastatic prostate cancer. *Eur J Nucl Med Mol Imaging* 2016;43:42.
33. Kratochwil C, Giesel FL, Bruchertseifer F, et al. ( $^{213}\text{Bi}$ )-DOTATOC receptor-targeted alpha-radionuclide therapy induces remission in neuroendocrine tumours refractory to beta radiation: A first-in-human experience. *Eur J Nucl Med Mol Imaging* 2014;41:2106.